Journal of Alloys and Compounds, 2012. **541**(0): p. 177-185.
doi: 10.1016/j.jallcom.2012.07.022

Bey Vrancken[a]
Lore Thijs[a]
Jean-Pierre Kruth[b]
Jan Van Humbeeck[a]

[a] *KU Leuven, Department of Metallurgy and Materials Engineering, Leuven, Belgium*

[b] *KU Leuven, Department of Mechanical Engineering, Leuven, Belgium*

Heat treatment of Ti6Al4V produced by Selective Laser Melting: Microstructure and Mechanical properties

Abstract

The present work shows that optimization of mechanical properties via heat treatment of parts produced by Selective Laser Melting (SLM) is profoundly different compared to conventionally processed Ti6Al4V. In order to obtain optimal mechanical properties, specific treatments are necessary due to the specific microstructure resulting from the SLM process. SLM is an additive manufacturing technique through which components are built by selectively melting powder layers with a focused laser beam. The process is characterized by short laser-powder interaction times and localized high heat input, which leads to steep thermal gradients, rapid solidification and fast cooling. In this research, the effect of several heat treatments on the microstructure and mechanical properties of Ti6Al4V processed by SLM is studied. A comparison is made with the effect of these treatments on hot forged and subsequently mill annealed Ti6Al4V with an original equiaxed microstructure. For SLM produced parts, the original martensite α' phase is converted to a lamellar mixture of α and β for heat treating temperatures below the β-transus (995°C), but features of the original microstructure are maintained. Treated above the β-transus, extensive grain growth occurs and large β grains are formed which transform to lamellar α+β upon cooling. Post treating at 850°C for two hours, followed by furnace cooling increased the ductility of SLM parts to 12.84 ± 1.36 %, compared to 7.36 ± 1.32 % for as-built parts.

Keywords: Metals and alloys; Powder metallurgy; Rapid solidification; Mechanical Properties; Microstructure;

Journal of Alloys and Compounds, 2012. **541**(0): p. 177-185.
doi: 10.1016/j.jallcom.2012.07.022

1. Introduction

The Selective Laser Melting (SLM) process is one of recently developed additive manufacturing techniques that emerged in the late 1980s and early 1990s [1-3]. The process has been described in detail elsewhere and the reader is referred to Ref. [3] for more detail.

SLM offers several advantages compared to conventional production techniques, such as reduction of production steps, a high level of flexibility, a high material use efficiency and a near net shape production. Furthermore, hard materials or materials with a high melting point can be processed with SLM. Most important, because of the layer-wise building, SLM enables the production of parts with a high geometrical complexity. However, the unique conditions during the SLM process give rise to some problems. Because of the short interaction times and accompanying highly localized heat input, large thermal gradients exist during the process. These lead to the build-up of thermal stresses, while the rapid solidification leads to segregation phenomena and the development of non-equilibrium phases. Moreover, non-optimal scan parameters may cause melt pool instabilities during the process, which leads to an increased porosity and a higher surface roughness.

To ensure optimal building conditions, the influence of the different process parameters, such as layer thickness, scan spacing, scan strategy, laser power and scan speed on the microstructure and mechanical properties [4-8] and other properties such as the density and surface quality [9-12] have been investigated. Other research has focused on optimization and control of the process [13-15] and simulation of the melt pool behavior [16].

On the other hand, heat treatments of Ti6Al4V have been investigated extensively. Amongst others, attempts have been made to model the kinetics [17-19] and phase morphology [20-22], to measure the alpha fraction at high temperature [23] and to create a CCT diagram [24, 25]. However, the starting material is always in the mill annealed condition (i.e. with equiaxed alpha grains) or has been subjected to some degree of previous deformation. Mill annealing is performed on heavily deformed Ti6Al4V, in which the breakup of the α plates leads to a recrystallization of the α phase. This results in an equiaxed microstructure and a small, general improvement of the mechanical properties.

As is shown in previous studies [4, 7], the microstructure of Ti6Al4V processed by SLM consists of a fine acicular martensite called the α' phase. Mechanical properties of these SLM parts are a high yield stress (about 1 GPa), a high ultimate tensile strength but a relatively low ductility (less than 10%). To improve the ductility of Ti6Al4V products manufactured by SLM, and to achieve a variety of desired mechanical properties for particular applications, suitable post-production heat treatments must be elaborated. Furthermore, these treatments allow the reduction of thermal stresses that have been built up during the process. Only limited research has been performed on this topic [5, 26, 27], and has mainly been observational. In this paper, the different response of SLM parts on generally applied titanium heat treatments is studied and the influence of time, temperature and cooling rate is distinguished. It appears that standard treatments for bulk alloys are not optimal for SLM produced parts and have to be adapted for optimal mechanical properties.

Journal of Alloys and Compounds, 2012. **541**(0): p. 177-185.
doi: 10.1016/j.jallcom.2012.07.022

2. Materials and methods

Extra-low interstitial Ti6Al4V (Grade 23) powder was used as a base material for the SLM process. The powder is produced via the plasma-atomization process by Raymor Industries. The equiaxed Ti6Al4V (Grade 5) was hot forged and mill annealed. This material will further be addressed as the reference material.

All SLM parts were produced on the in-house developed LM-Q SLM machine of the PMA Division of the Department of Mechanical Engineering, KU Leuven. This machine is equipped with an IPG YLR-300 SMYb:YAG fiber laser, with a wavelength of 1070 nm, a maximum power of 300 W in continuous laser mode and a spot size of 52 µm. For more details, the reader is referred to Ref. [13].

Samples were produced with a scanning speed v of 1600 mm/s, a laser power P of 250 W, 60 µm hatch spacing h (the distance between two adjacent scan vectors) and a 30 µm layer thickness t. Layers were scanned using a continuous laser mode according to a zigzag pattern, which was rotated 90° between each layer. This parameter set was determined to obtain fully dense, good quality Ti6Al4V products.

Before heat treating, samples were enclosed in a vacuum quartz tube, with vacuum better than 10^{-6} mbar. Heat treatments were executed in a vertical tube furnace, with a heating rate of approximately 10°C/min. Three different cooling regimes were applied. Furnace cooling was attained by turning the heating off, taking approximately two hours to cool from 800°C to 500°C, which corresponds to an average cooling rate of 0.04°C/s, and air cooling by cooling the quartz tube in a room temperature environment, leading to an approximate cooling rate of 7°C/s [22, 25]. To water quench, the tube was dropped and broken in a water reservoir, cooling the samples to room temperature in a matter of seconds. Some heat treatments were performed purely for microstructural examination.

Four tensile test samples of the SLM material were tested for each treatment to determine the mechanical properties. These samples were built as rectangular beams from which the final shape was cut by wire EDM. Tensile tests were performed according to ASTM E 8M at a strain rate of 1 mm/min. Displacements were measured using an extensometer with a 25 mm gauge length. Yield stress and Young's modulus were determined according to ASTM E 111. Samples were tested perpendicular to the build direction.

Examination of the microstructure occurred after grinding with SiC grinding paper up to a fine 4000 grit size, and polished with SiO_2 suspension. To reveal the microstructure, samples were etched with a 50 ml H_2O, 25 ml HNO_3 and 5 ml HF solution. Because of the anisotropic build process, two cross-sections are always considered. One is a side view parallel to the build direction, and the other is a top view, perpendicular to the build direction. Micrographs were taken using an Axioskop 40 Pol/40 A Pol microscope. A Philips SEM XL30 FEG was used for the examination of fracture surfaces and higher resolution micrographs. Texture and crystallographic orientation were examined by X-ray diffraction (XRD) and electron backscattered diffraction (EBSD). EBSD uses inelastic scattering of electrons to generate Kikuchi patterns which can be compared to Kikuchi patterns of known crystal orientations.

Dimensions of microstructural features are measured using the line intercept method described in ASTM E112. Circles are used instead of straight lines when measuring the size of elongated features such as needles and lamellae. Lamella size is reported as the true thickness, which is taken as half of the measured thickness, according to Ref [28]. All measurements of these properties are given with a 95% confidence interval.

3. Results

3.1 Microstructure

Figure 1a and 1b show respectively a top and side view of non-heat treated Ti6Al4V, produced by SLM. The top view indicates that a fully acicular α' martensitic microstructure is developed during the SLM process. XRD measurements did not indicate the presence of β phase. Due to the alternating scan pattern and the 90° shift between subsequent layers, a chessboard pattern appears. The squares are about 60 µm wide, corresponding to the hatch spacing of 60 µm used to build the part. At a smaller magnification, the side view reveals long, columnar grains which are oriented more or less in the building direction. These are identified as prior β grains which grow epitaxially during the process, up to several millimeters in length. The average width of the β grains is 55.5 ± 5 µm, which is close to the hatch spacing. A more comprehensive overview of the microstructure obtained by SLM is given by Ref. [7].

The reference material, shown in Figure 1c, consists of equiaxed α grains with 10.7 ± 0.9% β phase at the grain boundaries, as determined by pixel count of SEM images. A slight anisotropy exists in the reference material, with the α grains measuring 16.2 ± 2.6 µm in one direction and only 11.6 ± 1.7 µm in the perpendicular direction. This is attributed to the hot forging this material has been subjected to.

Journal of Alloys and Compounds, 2012. **541**(0): p. 177-185.
doi: 10.1016/j.jallcom.2012.07.022

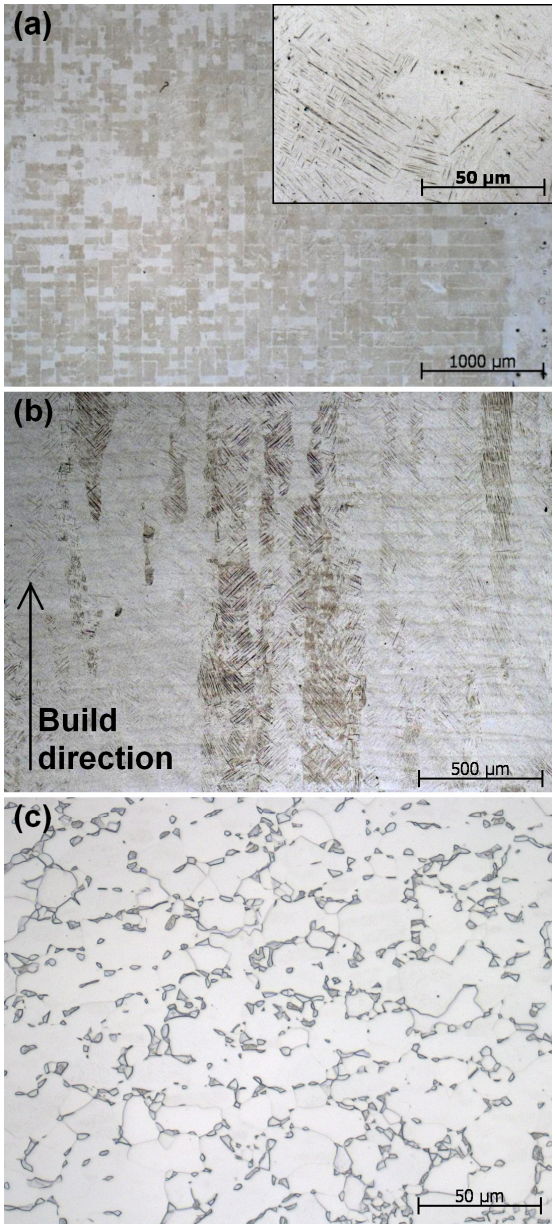

Figure 1 Top (a) and side (b) view of untreated Ti6Al4V produced by SLM. (c) Original microstructure of the reference material. The microstructure in (a) and (b) is fully martensitic. In (c), the α phase is lighter and the β phase darker.

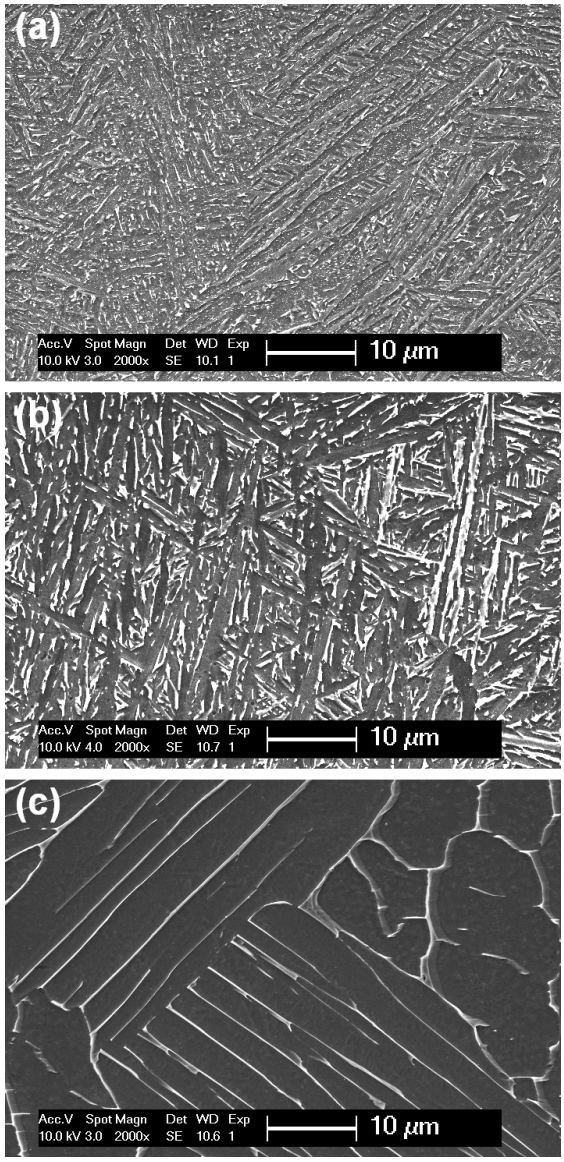

Figure 2 Microstructure of Ti6Al4V produced by SLM after heat treating at different temperatures for two hours, followed by FC. (a) 780°C and (b) 843°C below the β transus, (c) 1015°C above the β transus. Lighter zones are β phase, the dark phase is the α phase.

3.1.1 Influence of temperature

Microstructures of the *SLM material* after heat treating at different temperatures are shown in Figure 2. After two hours at 780°C, the fine martensitic structure has been transformed to a mixture of α and β, in which the α phase is present as fine needles (Figure 2a). The long, columnar grains remain visible in the side view of the material.

Journal of Alloys and Compounds, 2012. **541**(0): p. 177-185.
doi: 10.1016/j.jallcom.2012.07.022

At 850°C, the β-fraction at high temperature is larger, reducing the equilibrium α-fraction from approximately 87% at 780°C to 73% at 850°C and 23% at 950°C [20, 23]. From comparison of Figure 2a with Figure 2b, it is clear that the α plates are significantly coarser for higher temperatures. This observation corresponds to the FE calculations performed by Katzarov *et al* [20], where the α-β morphology was predicted to be coarser for higher holding temperatures beneath the β transus. The effect of temperature for subtransus treatments is further discussed in section 4.

When heating above the β transus of 995°C, a fully homogenic, 100% β phase microstructure exists at high temperature. During furnace cooling, a lamellar α+β mixture is formed, as shown in Figure 2c.

Figure 3a shows the side view of SLM material after a heat treatment at 940°C, below the β transus. After heat treatment below the β transus and at sufficiently low cooling rates, the prior β grains are now even more visible due to the formation of a layer of grain boundary α and the more aggressive etching of the α+β mixture as opposed to the original α'. On the other hand, Figure 3b shows that the microstructure no longer contains long columnar prior β grains after treatment above the β transus, indicating extensive grain growth of the SLM material when heated above the β transus, up to the point of semi-equiaxed β grains. The length of the prior β grains seems unchanged but the width has increased and is now roughly 620 µm wide after 2 hours at 1015°C. A comparison of the microstructure of SLM material after sub- and super-transus treatments by Sercombe *et al* [26] led to similar results, as did work by Vilaro *et al* [27].

As the equilibrium fraction of β phase rises at high temperatures, the intergranular β phase in the *reference material* grows into equiaxed grains. Upon cooling, these β grains transform to lamellar α+β, leading to a duplex microstructure, seen in Figure 4. This microstructure consists of equiaxed α grains and lamellar transformed β grains. At higher heat treatment temperatures, the equilibrium volume fraction of β phase is higher, which ultimately leads to a higher fraction of lamellar α+β at room temperature. When heated above the β transus, grain growth of the β phase can take place, leading to large grains.

Reference material samples treated at 1015°C still showed a duplex microstructure whereas a 100% transformed β structure was expected. This is cause to believe that the β transus of the reference material is higher than 1015°C. When treated at 1040°C, the microstructure fully consists of transformed β grains with varying degrees of grain boundary α, depending on the cooling rate.

3.1.2 Influence of the residence time

The residence time at high temperature affects grain growth, with longer residence times leading to larger grains. An analogous remark can be made about the heating rate. The time at high temperature and the heating rate are however of minor importance compared to the temperature for Ti6Al4V SLM parts when treated below the β transus. Both the α and the β phase will tend to coarsen but will hinder each other, hereby limiting grain growth. This effect diminishes as the temperature rises closer to the β transus and the α fraction decreases. The influence of the residence time will thus increase for higher temperatures in the α + β range.

Journal of Alloys and Compounds, 2012. **541**(0): p. 177-185.
doi: 10.1016/j.jallcom.2012.07.022

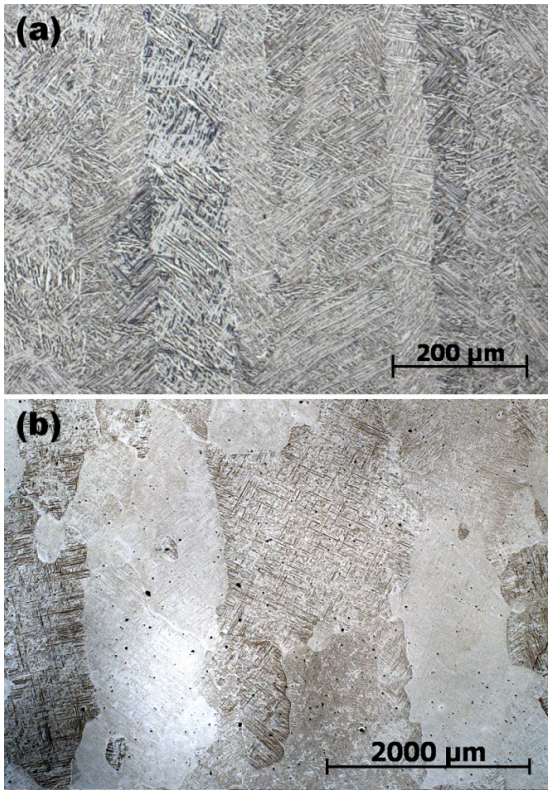

Figure 3 Side view of SLM material (a) after 1h at 940°C followed by 2h at 650°C, illustrating the long columnar prior β grains. After heat treatment, a lamellar mixture of α and β is present inside the columnar prior β grains. (b) After 1015°C, 2h, WQ, indicating the extensive growth of the columnar grains. Due to the water quench, the microstructure is fully martensitic. Notice the different scales.

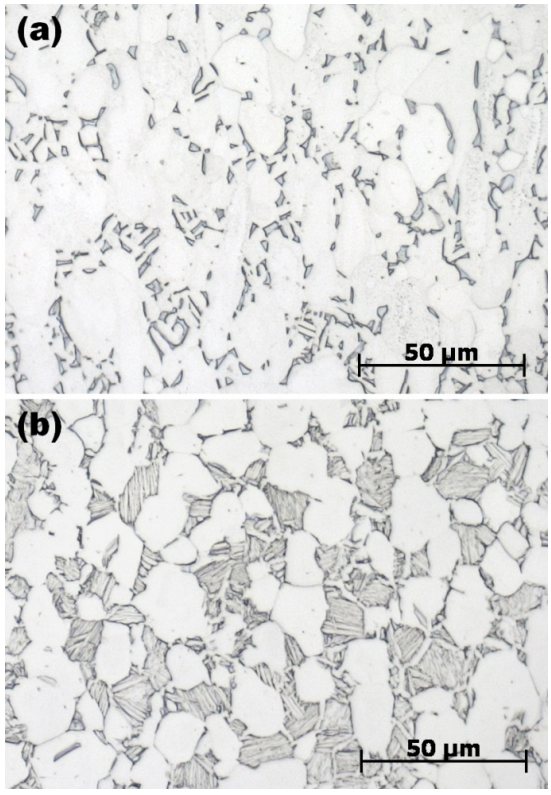

Figure 4 Duplex microstructure of the reference material consisting of equiaxed α grains and lamellar α+β. (a) two hours at 780°C, followed by furnace cooling and (b) one hour at 940°C, followed by air cooling to 650°C. The α phase is light, the β phase is dark. Notice the increase in lamellar fraction when treated at a higher maximum temperature.

Further evidence is provided in Figure 5, where the microstructure of SLM material is compared after two and twenty hours at 940°C, below the β transus. The α phase has started to globularize at some locations as indicated by the arrows in Figure 5b, whereas the majority of the section is similar to that after two hours. The α plates are 2.23 ± 0.12 µm wide after two hours and have coarsened to an average width of 2.80 ± 0.16 µm after twenty hours.

Previous research suggests that to achieve 50% globularization of the α phase at 955°C, a residence time of approximately 8 hours is necessary [17]. However, the starting material was originally equiaxed and deformed to local strains of 0.49, with a microstructure resembling elongated α grains rather than a lamellar structure. For finer, lamellar or platelike structures, it is expected that the time for globularization is drastically increased.

Journal of Alloys and Compounds, 2012. **541**(0): p. 177-185.
doi: 10.1016/j.jallcom.2012.07.022

The residence time is more important when heat treating above the β transus. Consisting of a single phase, grain growth can now take place unhindered and fast, considering the high temperatures. As the size of α colonies is limited to the β grain size, larger colonies are possible for longer residence times. From Figure 6, it is clear that the α colonies are larger after prolonged residence times. Lütjering [29] showed that the α colony size is a determining factor for the mechanical properties. As such, the residence time is an important parameter during β annealing.

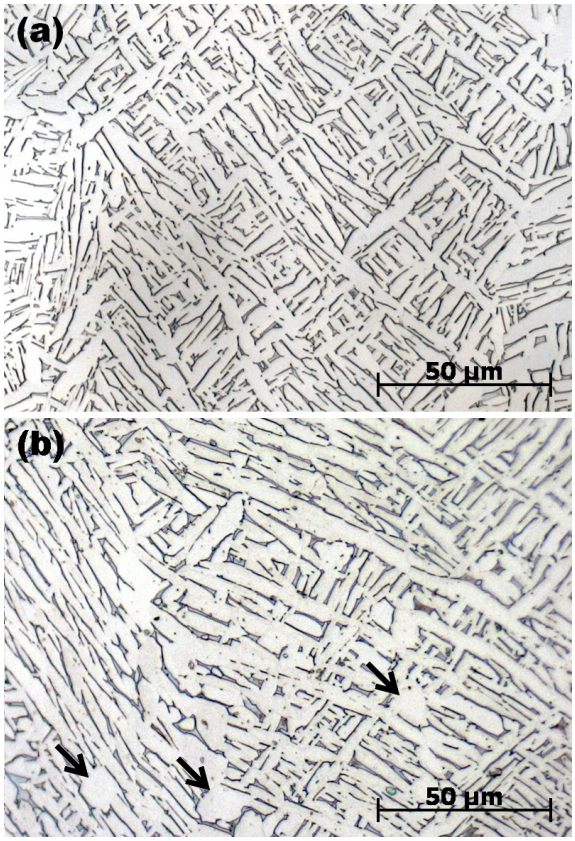

Figure 5 Comparison of the similarity in α plate size after (a) two hours at 940°C and (b) twenty hours at 940°C, followed by furnace cooling. The α phase is light, β is dark. The arrows in (b) indicate globularized α grains.

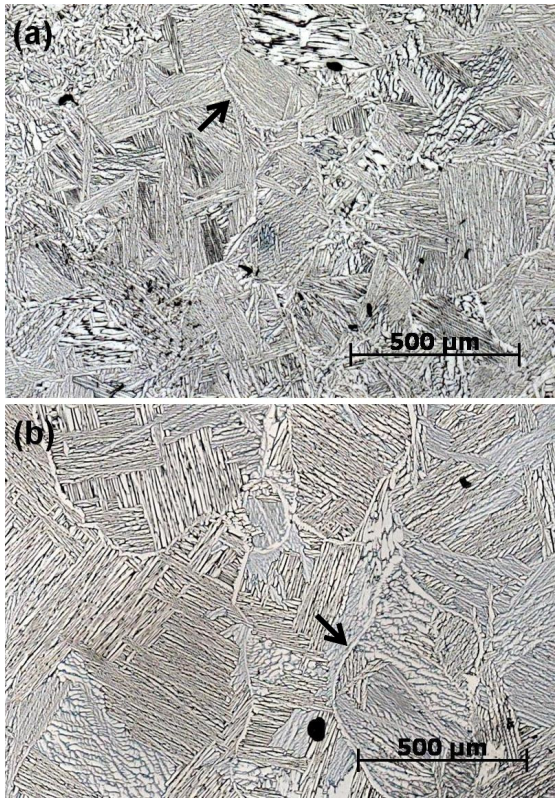

Figure 6 Illustration of the smaller α colony size after (a) two hours at 1020°C compared to after (b) twenty hours at 1040°C, followed by furnace cooling. The α phase is light, β is dark. The arrows indicate grain boundary α.

3.1.3 Influence of the cooling rate

In Figure 7, the microstructure of *SLM produced parts* after two hours at 850°C is compared for different cooling rates. These structures all look alike, and the α needle width is similar for all three, measuring 1.27 ± 0.13 µm after furnace cooling, 1.22 ± 0.09 µm after air cooling and 1.16 ± 0.13 µm after water quenching. Since the α fraction at 850°C is fairly large (73%, [20, 23]), the influence of the cooling rate is minimal. With rising maximum temperature, the amount of primary α that is still present at high temperature decreases and the influence of the cooling rate increases. This is apparent

Journal of Alloys and Compounds, 2012. **541**(0): p. 177-185.
doi: 10.1016/j.jallcom.2012.07.022

from needle size measurements after treatment at 950°C with different cooling rates. At this temperature, the α phase volume fraction is reduced to 23% and single α plates can now grow to a larger extent. The effect of cooling rate is now larger, leading to needle sizes of 1.48 ± 0.14 after water quenching, 1.57 ± 0.21 after air cooling and 2.23 ± 0.12 after furnace cooling. During both air cooling and water quenching the cooling rate is too high for significant grain growth to occur. Low cooling rates, such as during furnace cooling, allow the grains to grow during cooling.

When treated above the β transus, the cooling rate is the most important parameter that determines the final dimensions of the α phase and even the morphology [22, 29]. At high cooling rates, the large undercooling leads to the formation of many α nuclei resulting in smaller α colony size and a finer spacing between individual α plates. Furnace cooling results in lamellar α+β and air cooling results in an α-Widmanstätten microstructure or basket weave structure. The cooling rate during water quenching is higher than 410°C/s, leading to α' martensite [24].

The microstructure of the reference material displays a predictable dependency on the cooling rate: upon cooling, the transformation of equiaxed β grains that exist at high temperatures produces lamellar α+β. The lamellar spacing is dependent on the cooling rate, and decreases with increasing cooling rate. The thickness of the grain boundary α is also dependent on the cooling rate, decreasing with increasing cooling rate. When cooled from above the β transus, the cooling rate determines the size of the α colonies. The maximum size of an α colony is limited by the size of the β grain in which it originates [30].

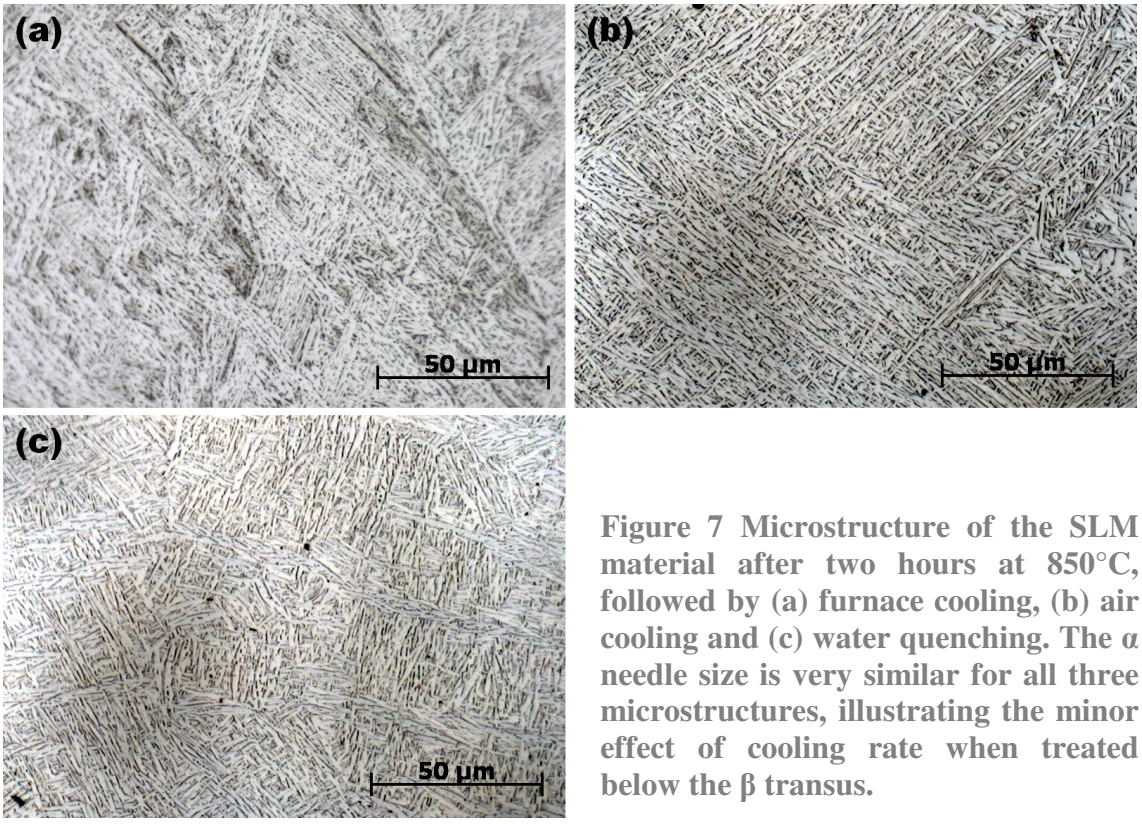

Figure 7 Microstructure of the SLM material after two hours at 850°C, followed by (a) furnace cooling, (b) air cooling and (c) water quenching. The α needle size is very similar for all three microstructures, illustrating the minor effect of cooling rate when treated below the β transus.

Journal of Alloys and Compounds, 2012. **541**(0): p. 177-185.
doi: 10.1016/j.jallcom.2012.07.022

3.2 Mechanical Properties

The mechanical properties of untreated SLM and reference material are shown in Figure 8 and are listed in Table 1. Three differences should be noted. First, the Young's modulus of the SLM material is slightly lower than that of the reference material. This is most likely caused by texture, which will be discussed in section 4. Second, the SLM material is much stronger than the reference material. This is true for all material processed by SLM because the rapid cooling conditions always lead to a fine microstructure. Third, because of the fine lamellar structure, the fracture strain is much lower compared to the equiaxed reference material. Note that the yield and ultimate strength of the reference material differ by only 50 MPa, indicating low strengthening by deformation.

	E [GPa]	σ_y [MPa]	UTS [MPa]	$\varepsilon_{fracture}$ [%]
SLM	109.2 ± 3.1	1110 ± 9	1267 ± 5	7.28 ± 1.12
Reference	120.2 ± 1.9	960 ± 10	1006 ± 10	18.37 ± 0.88

Table 1 Mechanical properties of untreated SLM and reference material.

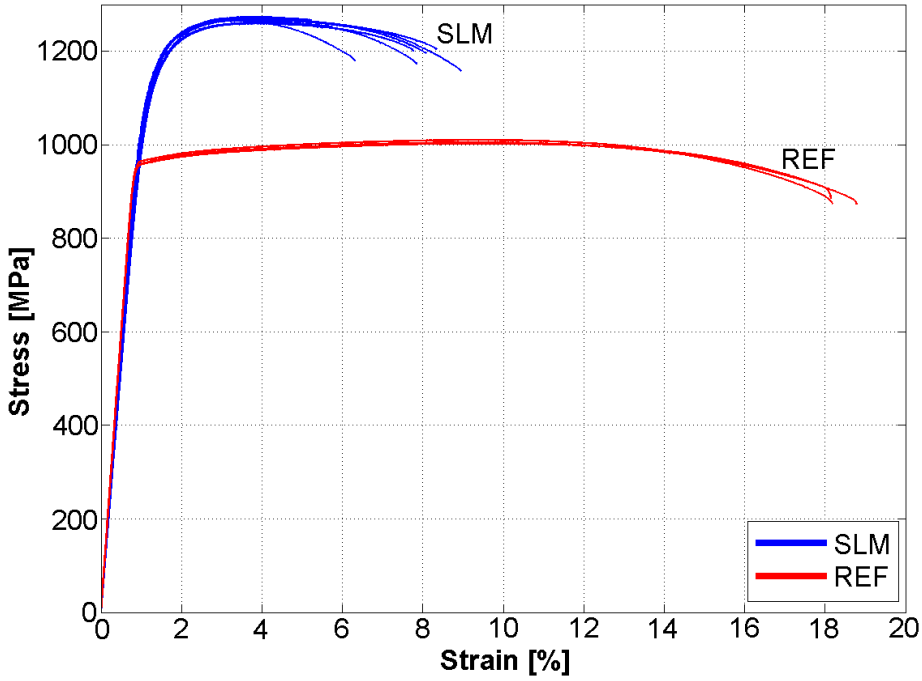

Figure 8 Stress-strain curves for untreated SLM material and reference material.

An overview of results after heat treatments of the SLM material is given in Table 2. From these results, treatment two (2h at 850°C, followed by furnace cooling) and seven (1h at 940°C, followed by air cooling and tempering for 2h at 650°C and air cooling) seem to produce the best overall results. Both of these treatments reach temperatures relatively high in the α+β zone and maintain some α at high temperature. A previous study on increasing the ductility of Ti6Al4V produced by SLM [5] produced the same mechanical properties as were obtained after treatment two, but did not state the heat treatment parameters that were used. The microstructure however differed to some extent, with some globular α being reported.

Journal of Alloys and Compounds, 2012. **541**(0): p. 177-185.
doi: 10.1016/j.jallcom.2012.07.022

Nr.	T [°C]	t [h]	Cooling Rate	E [GPa]	σ_y [MPa]	UTS [MPa]	$\varepsilon_{fracture}$ [%]
1	*540*	*5*	*WQ*	112.6 ± 30.2	1118 ± 39	1223 ± 52	5.36 ± 2.02
2	*850*	*2*	*FC*	114.7 ± 3.6	955 ± 6	1004 ± 6	12.84 ± 1.36
3	*850*	*5*	*FC*	112.0 ± 3.4	909 ± 24	965 ± 20	- (premature failure)
4	*1015* *followed by* *843*	*0.5* *2*	*AC* *FC*	114.9 ± 1.5	801 ± 20	874 ± 23	13.45 ± 1.18
5	*1020*	*2*	*FC*	114.7 ± 0.9	760 ± 19	840 ± 27	14.06 ± 2.53
6	*705*	*3*	*AC*	114.6 ± 2.2	1026 ± 35	1082 ± 34	9.04 ± 2.03
7	*940* *followed by* *650*	*1* *2*	*AC* *AC*	115.5 ± 2.4	899 ± 27	948 ± 27	13.59 ± 0.32
8	*1015* *followed by* *730*	*0.5* *2*	*AC* *AC*	112.8 ± 2.9	822 ± 25	902 ± 19	12.74 ± 0.56

Table 2 Mechanical properties of the SLM material after different heat treatments. WQ = water quenching. AC = air cooling. FC = furnace cooling. Treatment six to eight are well known titanium heat treatments [30]. Samples for treatment three were built in a different batch in which building errors are present, which led to premature failure of the components.

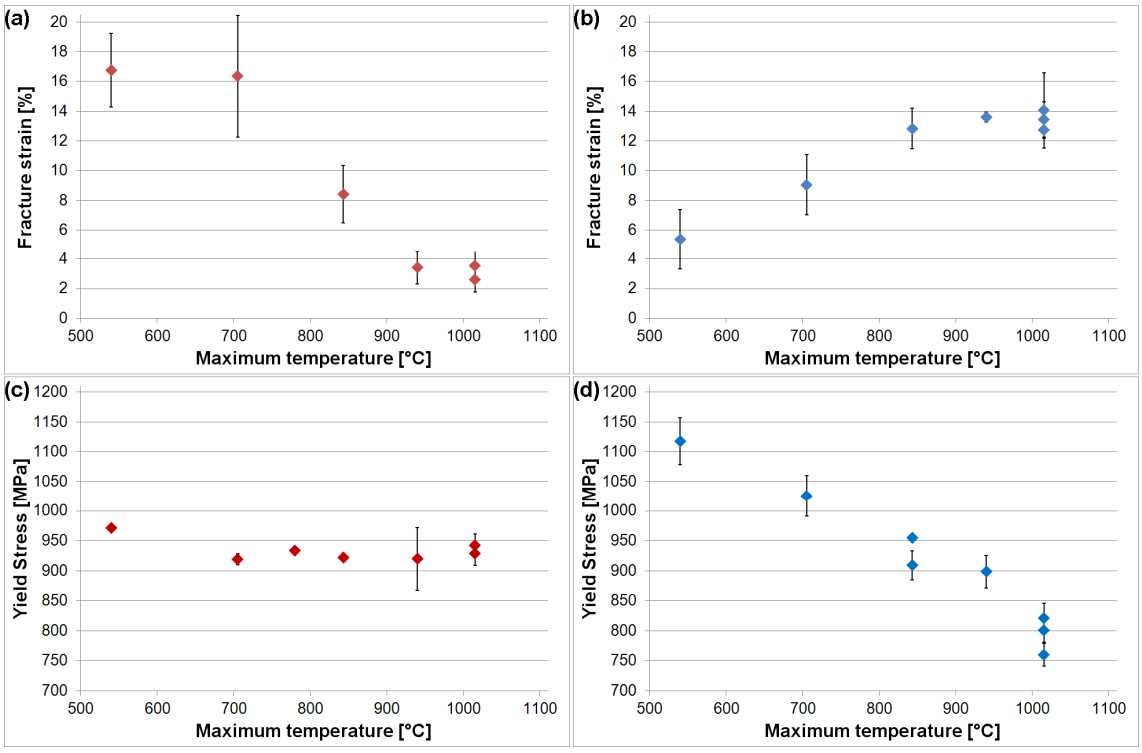

Figure 9 Fracture strain and yield stress of the reference (a and c) and SLM material (b and d) in function of the maximum heat treating temperature. Results of all heat treatments are shown, regardless of cooling rate. All super-transus treatments used either AC or FC from the β range.

Journal of Alloys and Compounds, 2012. **541**(0): p. 177-185.
doi: 10.1016/j.jallcom.2012.07.022

The mechanical properties differ greatly after the various heat treatments. When plotting the maximum strain and yield stress in function of the maximum heat treating temperature, as in Figure 9, certain tendencies can be noticed, regardless of the cooling rate. First, the fracture strain of the *SLM material* goes up with rising maximum temperature, from 9.04 ± 2.03 after heat treatment six (max. 705°C) to 14.06 ± 2.53 after heat treatment five (max. 1020°C). The low fracture strain after treatment one could be due to the formation of very fine Ti_3Al precipitates, although these were not visible by SEM. These precipitates are known to occur for holding temperatures below 550°C [29]. In contrast to the results in Ref. [5] and [27], where yield stress and UTS values are reported to increase, the yield stress and UTS decrease after heat treatment, as was expected due to coarsening of the microstructure compared to the original fine α' martensite. The yield stress decreases from 1026 ± 35 after heat treatment six to 760 ± 19 after heat treatment five. The difference between the yield stress and the ultimate tensile strength, which is more than 200 MPa for as built SLM parts remains stable at about 60 MPa after heat treatment. This means that after heat treatment, the SLM material partially loses the ability to strengthen by deformation.

The response of the *reference material* to the heat treatments is completely different and is shown in Figure 9a and 9c. It is clear that the yield stress does not change significantly after the different heat treatments. This is due to the competitive growth of both the α and β grains at high temperature, thus effectively hindering each other to grow. This leads to similar grain sizes after each treatment. Following the Hall-Petch relation, the yield stresses after the treatments do not differ largely. As illustrated in Figure 9a, the fracture strain of the reference material decreases drastically with rising heat treatment temperature. This is attributed to the development of a duplex microstructure, as will be discussed in section 4.

Standard heat treatments for Ti6Al4V were also performed on SLM produced parts, including the regular 'mill anneal' for cold deformed Ti6Al4V (treatment six, Table 2), duplex anneal (treatment seven) and a β anneal (treatment eight) [30]. β annealing normally leads to improved fracture toughness but a lower ductility.

From the results in Table 2 and Figure 9, it can be seen that these treatments did not produce the expected results, neither for the SLM material nor for the equiaxed reference material. This is because these treatments are designed for specific purposes, starting from a specific microstructure, for example the heavily deformed structure before mill annealing. The reference material already consists of the equiaxed microstructure desired after treatment six, and the SLM material consists of a very fine, needle-like martensite rather than a heavily deformed mixture of α and β. The maximum temperature of treatment six is too low to lead to any significant changes. Treatment seven however is executed at high temperature below the β transus. As debated earlier in section 3.1, temperature is of major importance when treated below the β transus, which is why this treatment led to favorable results for SLM produced parts. Considering the β anneal, the ductility of the SLM material is increased rather than decreased. β annealing an equiaxed microstructure transforms it to a lamellar α+β, Widmanstätten α or martensitic α' microstructure, depending on the cooling rate. All of these structures have a lower ductility and because of the lamellar structure, the crack path is deviated during fracture. This leads to an increased fracture toughness [31].

However, during β annealing of SLM material, the α' structure transforms into a coarser lamellar structure, increasing rather than decreasing the ductility.

4. Discussion

Comparing the ductility of the reference material and the SLM material after heat treatment as in Figure 9, the fracture strain of the SLM material increases with rising maximum temperature, whereas the reference material loses up to 86% of its ability to deform. This is most likely caused by the formation of a duplex structure in the reference material, in which the α stabilizing alloying elements are mostly located in the primary α grains. The α phase in the lamellar section is then relatively poor in alloying elements, causing a great difference in strength between the α and β lamellae. This causes rapid formation of cracks and early failure of the material [29, 32]. Because there are no equiaxed α grains, this segregation effect does not occur in the SLM material.

For the *reference material*, the maximum heat treating temperature determines only the final lamellar α+β fraction when treated below the β transus. Since the equilibrium β fraction is higher at temperatures closer to the β transus, and these equiaxed β grains transform to lamellar α+β upon cooling, a higher heat treating temperature will result in a larger lamellar fraction at room temperature. The lamellar spacing is determined by the cooling rate, with higher cooling rates resulting in a finer lamellar spacing.

The final spacing of the microstructural features in the *SLM material* is not primarily dependent on the cooling rate, but on the maximum temperature for heat treatments in the intermediate α+β range. The SLM material originally consists of fine α' needles. When heated, α phase is nucleated along the α' boundaries and vanadium atoms are expulsed, leading to the formation of β at the α phase boundaries [33]. At high temperatures, only a fraction of the original amount of nuclei is still present, since the equilibrium α fraction is lower, but still considerable (e.g. 73% at 850°C, 23% at 950°C [20, 23]). Originating from a fine α' microstructure, these α phase nuclei are scattered at high temperature. For higher temperatures, less nuclei are present and they can coarsen to a greater extent before interaction with other plates will occur.

Thus, for intermediate temperatures in the α+β range, the size of the α needles at room temperature is mostly determined by the number of α needles at high temperature, which in turn is closely related to the temperature. At high temperatures in the α+β range, the effect of cooling rate becomes more distinct, with furnace cooling leading to a coarser microstructure.

From comparison between the microstructure of the *SLM material* treated below the β and above the β transus it is clear that the SLM footprint is erased for temperatures above the β transus. During heating, the SLM material gradually transforms back to the original columnar β grains. However, these columnar grains are no longer present after cooling from above the β transus. Instead, the microstructure consists of α colonies inside large, semi-equiaxed, previous β grains. Following the Burgers relation given in Equation 1 [34], a Widmanstätten structure is formed due to the preferential growth of the α phase parallel to the (110) family of crystallographic planes of the β phase [22, 24] for intermediate cooling rates between air cooling and furnace cooling [30].

Journal of Alloys and Compounds, 2012. **541**(0): p. 177-185.
doi: 10.1016/j.jallcom.2012.07.022

$$(110)_\beta \leftrightarrow (0001)_\alpha$$
$$\langle 1\bar{1}1\rangle_\beta \leftrightarrow \langle 11\bar{2}0\rangle_\alpha \quad (1)$$

Because growth along these planes is faster, the α phase is formed as flat plates or needles. The large difference in size and shape of the transformed β grains after treatment above 995°C compared to the original columnar β grains present in as built SLM parts indicates extensive grain growth at temperatures above the β transus, up to the point where the columnar grains resemble a coarse equiaxed microstructure with large grains several millimeters long and approximately 620 µm wide. This is illustrated by Figure 10, where EBSD orientation maps of the microstructure after treatments below (a) and above (b) the β transus are shown. The black lines are intensified drawings of the prior β grain boundaries.

During solidification, the bcc β phase preferentially grows in the <100> direction, giving rise to the long, columnar prior β grains as described by Thijs *et al* [7] and Kobryn *et al* [35]. The <100> direction of each of these columnar grains is thus oriented quasi parallel to the build direction, and the rotation of the grain around this direction is considered to be random, causing the presence of a fiber-like texture. Due to the fast cooling, the β phase then transforms to the α' phase according to the Burgers relation given by Equation 1. The texture of the parent β phase is transmitted to a texture of the α phase, as can be seen in the $<10\bar{1}2>$ pole figure of the top view of untreated SLM material in Figure 11a.

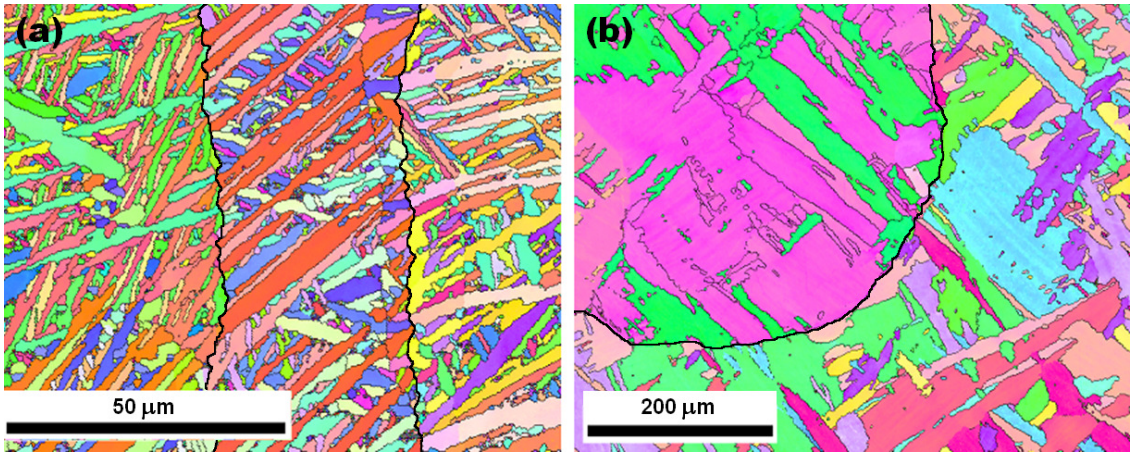

Figure 10 EBSD orientation maps of a) SLM material after two hours at 850°C, followed by furnace cooling. b) SLM material after half an hour at 1020°C, followed by two hours at 730°C and air cooling. Contrast is provided by the different orientations of the α phase, while the β phase is present as a thin layer between the α phase. Notice the different scale. The build direction for both images is vertical.

Journal of Alloys and Compounds, 2012. **541**(0): p. 177-185.
doi: 10.1016/j.jallcom.2012.07.022

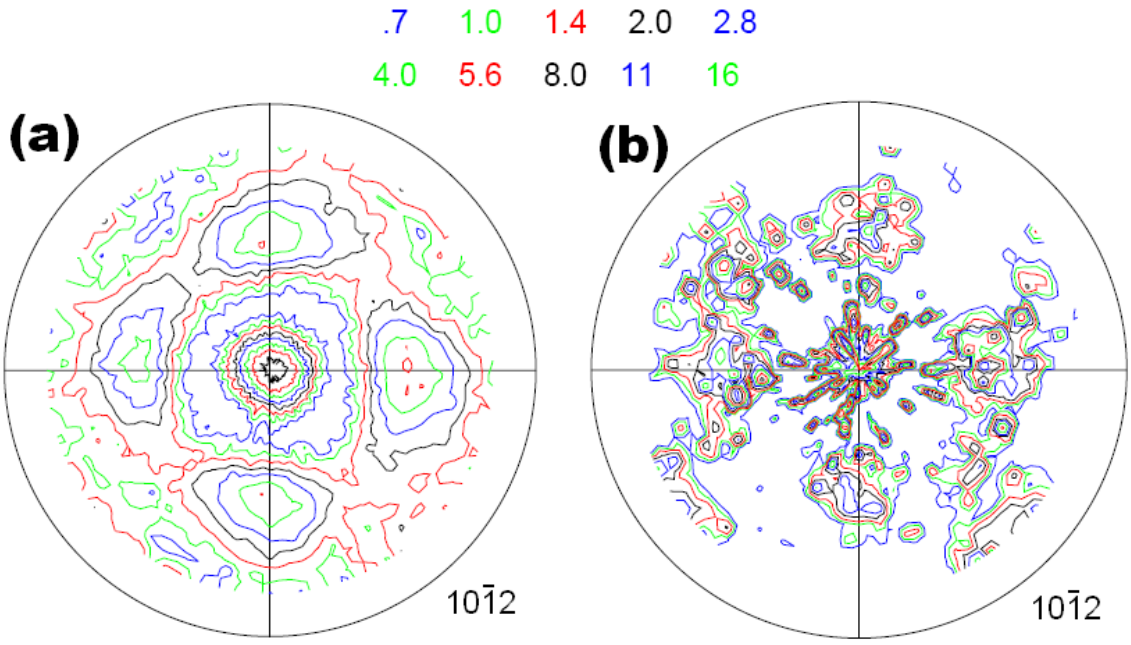

Figure 11 HCP $<10\bar{1}2>$ pole figures of (a) the untreated SLM material and (b) the SLM material heat treated above the β transus, for 20 hours at 1040°C, followed by furnace cooling. In (a), the texture is present in the α' phase which has a similar crystal lattice as the α phase. In (b) the texture in the α phase is shown.

When treated above the β transus, the β grains in the SLM material will grow and the texture is maintained, as seen in the pole figure in Figure 11b. The texture after homogenization in the β field is not as distinguished because of the extremely large grain sizes after prolonged treatment above the β transus, causing large intensity peaks for one individual grain.

Due to the texture in the build direction, it is suspected that mechanical properties of SLM parts are different parallel to the build direction compared to perpendicular to the build direction. For an austenitic stainless steel, Meier [36] reported the tensile strength and elongation to be lower for samples tested in the build direction compared to horizontally built specimens.

5. Conclusion

Several heat treatments were performed on Ti6Al4V produced by SLM with an original α' microstructure. The influence of temperature, time and cooling rate were distinguished. When heated, α phase is precipitated at the α' boundaries. At maximum temperatures below the β transus, the mixture of α and β phase prevents grain growth and the original, columnar prior β grains remain visible after cooling. The width of the α plates after heat treatment is mainly dependent on the maximum temperature for sub-transus treatments, and primarily dependent on the cooling rate for super-transus treatments. The residence time and cooling rate do not have a significant influence for sub-transus treatments, although their influence increases when temperatures are closer to the β transus. When treated above the β transus, the columnar β grains grow extensively to form large, semi-equiaxed β grains. For FC, AC and WQ samples, the β grains then transform to lamellar α+β, α-Widmanstätten colonies or α' martensite,

respectively. The residence time influences the final dimensions of the transformed β grains.

Mechanical properties are very much dependent on the maximum heat treatment temperature. With rising maximum temperature, σ_y and UTS decline and the fracture strain rises because of the transformation of the fine α' needles to a more coarse mixture of α and β. Overall best results are obtained after two hours at 850°C, followed by furnace cooling, or one hour at 940°C, air cooling and tempering for two hours at 650°C followed by air cooling. The results for all properties are well above ASTM Standards for forged (ASTM F1472) and cast Ti6Al4V (ASTM F1108). The importance of the initial microstructure cannot be stressed enough. Due to the very fine martensite, the kinetics are completely different as compared to treatment of equiaxed or heavily deformed microstructures. Consequently, application of standard heat treatments shows that these treatments do not lead to the usual or expected results. **Due to the specific process conditions and hence specific microstructure, SLM produced parts need to be treated differently than bulk alloy parts.**

For SLM produced Ti6Al4V parts, heat treating at intermediate to high temperatures below the β transus, followed by furnace cooling proved to be optimal for an overall optimization of tensile properties, with deformability levels safely above the prescribed standards and yield stress and UTS levels close to 1 GPa.

References

[1] G. N. Levy. The role and future of the Laser Technology in the Additive Manufacturing environment. Physics Procedia 5 (2010) 65-80.
[2] J. Kruth. Material Incress Manufacturing by Rapid Prototyping Techniques. CIRP Annals - Manufacturing Technology 40 (1991) 603-614.
[3] J. P. Kruth, G. Levy, F. Klocke and T. H. C. Childs. Consolidation phenomena in laser and powder-bed based layered manufacturing. CIRP Ann-Manuf. Technol. 56 (2007) 730-759.
[4] L. E. Murr, S. A. Quinones, S. M. Gaytan, M. I. Lopez, A. Rodela, E. Y. Martinez, D. H. Hernandez, E. Martinez, F. Medina and R. B. Wicker. Microstructure and mechanical behavior of Ti-6Al-4V produced by rapid-layer manufacturing, for biomedical applications. Journal of the Mechanical Behavior of Biomedical Materials 2 (2009) 20-32.
[5] L. Facchini, E. Magalini, P. Robotti, A. Molinari, S. Hoges and K. Wissenbach. Ductility of a Ti-6Al-4V alloy produced by selective laser melting of prealloyed powders. Rapid Prototyping J. 16 (2010) 450 - 459.
[6] L. Facchini, E. Magalini, P. Robotti and A. Molinari. Microstructure and mechanical properties of Ti-6Al-4V produced by electron beam melting of pre-alloyed powders. Rapid Prototyping J. 15 (2009) 171-178.
[7] L. Thijs, F. Verhaeghe, T. Craeghs, J. Van Humbeeck and J. P. Kruth. A study of the micro structural evolution during selective laser melting of Ti-6Al-4V. Acta Mater. 58 (2010) 3303-3312.
[8] E. Chlebus, B. a. KuÅºnicka, T. Kurzynowski and B. DybaÅ‚a. Microstructure and mechanical behaviour of Tiâ€•6Alâ€•7Nb alloy produced by selective laser melting. Mater. Charact. 62 (2011) 488-495.

[9] R. Morgan, C. J. Sutcliffe and W. O'Neill. Density analysis of direct metal laser re-melted 316L stainless steel cubic primitives. Journal of Materials Science 39 (2004) 1195-1205.
[10] I. Yadroitsev and I. Smurov. Surface Morphology in Selective Laser Melting of Metal Powders. Lasers in Manufacturing 2011: Proceedings of the Sixth International Wlt Conference on Lasers in Manufacturing, Vol 12, Pt A, vol. 12. Amsterdam: Elsevier Science Bv, 2011. p.264-270.
[11] E. Yasa, J. Deckers and J. P. Kruth. The investigation of the influence of laser re-melting on density, surface quality and microstructure of selective laser melting parts. Rapid Prototyping J. 17 (2011) 312-327.
[12] A. B. Spierings, N. Herres and G. Levy. Influence of the particle size distribution on surface quality and mechanical properties in AM steel parts. Rapid Prototyping J. 17 (2011) 195-202.
[13] J. Van Vaerenbergh. Process optimisation in Selective Laser Melting. vol. PhD. Twente: University of Twente, 2008.
[14] P. Mercelis and J. P. Kruth. Residual stresses in selective laser sintering and selective laser melting. Rapid Prototyping J. 12 (2006) 254-265.
[15] B. Vandenbroucke. Selective Laser Melting of Biocompatible Metals for Rapid Manufacturing of Medical Parts. vol. PhD. Leuven: KU Leuven, 2008.
[16] F. Verhaeghe, T. Craeghs, J. Heulens and L. Pandelaers. A pragmatic model for selective laser melting with evaporation. Acta Mater. 57 (2009) 6006-6012.
[17] N. Stefansson, S. Semiatin and D. Eylon. The kinetics of static globularization of Ti-6Al-4V. Metallurgical and Materials Transactions A 33 (2002) 3527-3534.
[18] S. Semiatin, N. Stefansson and R. Doherty. Prediction of the kinetics of static globularization of Ti-6Al-4V. Metallurgical and Materials Transactions A 36 (2005) 1372-1376.
[19] S. Malinov, Z. Guo, W. Sha and A. Wilson. Differential scanning calorimetry study and computer modeling of beta double right arrow alpha phase transformation in a Ti-6Al-4V alloy. Metallurgical and Materials Transactions a-Physical Metallurgy and Materials Science 32 (2001) 879-887.
[20] I. Katzarov, S. Malinov and W. Sha. Finite element modeling of the morphology of beta to alpha phase transformation in Ti-6Al-4V alloy. Metallurgical and Materials Transactions a-Physical Metallurgy and Materials Science 33 (2002) 1027-1040.
[21] S. Semiatin, S. Knisley, P. Fagin, D. Barker and F. Zhang. Microstructure evolution during alpha-beta heat treatment of Ti-6Al-4V. Metallurgical and Materials Transactions A 34 (2003) 2377-2386.
[22] F. J. Gil, M. P. Ginebra, J. M. Manero and J. A. Planell. Formation of alpha-Widmanstatten structure: effects of grain size and cooling rate on the Widmanstatten morphologies and on the mechanical properties in Ti6Al4V alloy. J. Alloys Compd. 329 (2001) 142-152.
[23] R. Pederson, O. Babushkin, F. Skystedt and R. Warren. Use of high temperature X-ray diffractometry to study phase transitions and thermal expansion properties in Ti-6Al-4V. Mater. Sci. Technol. 19 (2003) 1533-1538.
[24] T. Ahmed and H. J. Rack. Phase transformations during cooling in α+β titanium alloys. Materials Science and Engineering: A 243 (1998) 206-211.
[25] R. Dabrowski. The Kinetics of Phase Transformations During Continuous Cooling of Ti6Al4V Alloy from the Diphase α β Range. Archives of metallurgy and materials 56 (2011) 217-221.

[26] T. Sercombe, N. Jones, R. Day and A. Kop. Heat treatment of Ti-6Al-7Nb components produced by selective laser melting. Rapid Prototyping J. 14 (2008) 300-304.
[27] T. Vilaro, C. Colin and J. D. Bartout. As-Fabricated and Heat-Treated Microstructures of the Ti-6Al-4V Alloy Processed by Selective Laser Melting. Metall. Mater. Trans. A 42A (2011) 3190-3199.
[28] E. E. Underwood. Quantitative stereology. Addison-Wesley Educational Publishers Inc, 1970.
[29] G. Lütjering. Influence of processing on microstructure and mechanical properties of α+β titanium alloys. Materials Science and Engineering: A 243 (1998) 32-45.
[30] R. R. Boyer, G. Welsh and E. W. Collings. Materials properties handbook: Titanium alloys. ASM International, Materials Park: Ohio, 1994.
[31] G. Lütjering, J. C. Williams and A. Gysler. Microstructure and mechanical properties of titanium alloys. Titanium: Springer Science and Business Media, 2007. p.3540713972.
[32] E. Brandl. PhD Thesis. Brandenburg Technical University of Cottbus, 2010.
[33] F. X. Gil Mur, D. RodrÃ-guez and J. A. Planell. Influence of tempering temperature and time on the Î±â€²-Ti-6Al-4V martensite. J. Alloys Compd. 234 (1996) 287-289.
[34] W. Burgers. Physica 1 (1934) 561.
[35] P. A. Kobryn and S. L. Semiatin. Microstructure and texture evolution during solidification processing of Tiâ€“6Alâ€“4V. J. Mater. Process. Technol. 135 (2003) 330-339.
[36] H. Meier and C. Haberland. Experimental studies on selective laser melting of metallic parts. Materialwiss. Werkstofftech. 39 (2008) 665-670.